International Journal of Earth, Energy and Environmental Sciences
ISSN: 2517-942X
Vol:9, No:2, 2015

Analytical Development of a Failure Limit and Iso-Uplift Curves for Eccentrically Loaded Shallow Foundations

N. Abbas, S. Lagomarsino, S. Cattari

***Abstract*—**Examining existing experimental results for shallow rigid foundations subjected to vertical centric load (N), accompanied or not with a bending moment (M), two main non-linear mechanisms governing the cyclic response of the soil-foundation system can be distinguished: foundation uplift and soil yielding. A soil-foundation failure limit, is defined as a domain of resistance in the two dimensional (2D) load space (N, M) inside of which lie all the admissible combinations of loads; these latter correspond to a pure elastic, non-linear elastic or plastic behavior of the soil-foundation system, while the points lying on the failure limit correspond to a combination of loads leading to a failure of the soil-foundation system. In this study, the proposed resistance domain is constructed analytically based on mechanics. Original elastic limit, uplift initiation limit and iso-uplift limits are constructed inside this domain. These limits give a prediction of the mechanisms activated for each combination of loads applied to the foundation. A comparison of the proposed failure limit with experimental tests existing in the literature shows interesting results. Also, the developed uplift initiation limit and iso-uplift curves are confronted with others already proposed in the literature and widely used due to the absence of other alternatives, and remarkable differences are noted, showing evident errors in the past proposals and relevant accuracy for those given in the present work.

***Keywords*—**Foundation uplift, Iso-uplift curves, Resistance domain, Soil yield.

I. Introduction

THE foundation bearing capacity can be defined as the determination of all possible combinations of forces that can be supported by the foundation before soil failure.

Originally, a formula was developed in [1] to estimate the bearing capacity of a surface footing, referring to the ideal condition of strip footing subjected to vertical central load, on homogeneous soil, with a horizontal base and ground surface. Then, it was modified later; a reduction of the fundamental vertical centric load capacity was proposed in [2] by introducing empirical multiplication factors for each of its terms to consider footing shape, load inclination, eccentricity...

The shortcomings of conventional bearing capacity analyses based on well-known Brinch-Hansen's equation, led to a proposal [3], [4] that a better solution might be the useof the interaction diagram concept, a well-established procedure in structural engineering, especially noting the growing awareness, in the last decades, of the need to consider soil-foundation inelasticity in the seismic analysis and design projects. In fact, under seismic loading, foundation undergoes repetitive loading-unloading cycles leading to foundation rocking and/or sinking; the loading components and the corresponding reacting non-linear mechanisms change for each time step. Also, when rocking, the foundation base may detach from the underneath soil causing a reduction in the foundation bearing capacity.

Considering that the foundation behavior could greatly contribute to the response of the supported structure to seismic loading (usually referred to as soil–structure interaction (SSI) effects), an accurate "resisting domain" must be used to determine whether the foundation state, and hence, the load combinations, at each step of the loading-unloading cycles is still admissible or not. Also a detailed description of the type of non-linear mechanisms ruling at a determined loading/unloading step or causing the failure would be welcomed.

II. Objectives and Scope of Work

The objective of the current study is to provide a 2D resisting domain for shallow rigid foundation resting on a Winkler soil model, and subjected to a vertical centric component (N), with or without a bending moment component (M). The proposed resistance domain, defined by the interaction diagram in the two dimensional space of loading (N, M) is constructed analytically, based on mechanics. Original elastic limit, uplift initiation limit and iso-uplift limits are constructed inside this domain, giving a clear idea about the mechanisms activated for each combination of loads applied to the foundation, whether inside or at the limit of this domain.

III. Non-Linear Mechanisms Governing the Failure Domain

Footing may be subjected to vertical centric ($N\neq0$, $M=0$), or eccentric ($N\neq0$, $M\neq0$) loading, leading to its movement in the two dimensional plane of loading, and causing vertical displacements and/or rotation. Generally, the foundation is deemed to have failed if movement in any of these directions exceeds an acceptable threshold. Examining existing

N. Abbas is with the Civil Engineering Department, Lebanese University, Faculty of Engineering - Branch I, Tripoli, Lebanon (phone: 00961-71-542097; e-mail: nivine_abbas@ yahoo.com).

S. Lagomarsino and S. Cattari are with the Department of Civil, Environmental and Chemical Engineering, University of Genoa, Italy (e-mail: sergio.lagomarsino@unige.it, serena.cattari@unige.it).

experimental results for similarly loaded foundations, two main non-linear mechanisms governing the cyclic response of the soil-foundation system can be distinguished: foundation uplift, and soil plastification (soil yielding known also as foundation sinking).

A soil-foundation failure limit is defined as a resistance domain in the 2D load space (N,M) inside of which lie all the admissible combinations of loads, these latter correspond to a pure elastic, non-linear elastic or plastic behavior of the soil-foundation system, whereas the points lying on the failure limit correspond to a combination of loads leading to a total plastification of the soil under the foundation's effective contact area with soil (considering when uplift is activated or not).

These two main non-linear mechanisms are interpreted as follows:

- The foundation uplift mechanism: with prevailing action of the flexural moment, due to vertical load's eccentricity, the foundation extremity in tension is uplifted. Under cyclic loading, the alternating of uplift between the two foundation's extremities due to the change in loading direction causes the foundation rocking.
- The soil plasticity mechanism: representing the material nonlinearity and taking place with prevailing action of the vertical load, leading to sinking of the foundation in the soil (soil yielding). The soil plasticity starts when the elastic limit strength of the soil is reached.

IV. The Failure Domain: Derivation of State Equations

This diagram describes the domain of resistance of the foundation in the absence of horizontal load. Within the failure limit, different zones describing pure elastic, elastic with uplift, and plastic response of the soil-foundation system are elaborated, and several curves limiting these zones or describing a certain state of the foundation behavior are also constructed.

The assumption made in the derivation of the state equations are: (a) the axial load N is constant and acts at the center of the foundation. (b) The bending moment M acts about the transversal axis of the foundation and is computed about its center. (c) The foundation has a width B and a length L (L≥B).

From these assumptions an equivalent vertical constant load N with a varying eccentricity "e" can be applied, substituting the axial and moment load.

The basic idea is to integrate the distributed stresses under the foundation, for several generic foundation states, in order to find the expression of the moment M corresponding to each state as a function of the axial force N normalized by the vertical yielding force N_{max} , with $N_{max}= \sigma_y.L.B$ and σ_y is the soil yielding strength. This can be done simply noting that the expression of the moment can be written as M=N*e, where "e" is the eccentricity of the stresses diagram resultant R corresponding to each state.

Fig. 1 illustrates the generic foundation states proposed in this study and used to construct the failure domain. It shows a schematic of the assumed stress conditions for various footing states. These states correspond to different segments of the moment–rotation curve as shown in Fig. 2, this latter is divided in three segments: the first one represents pure elastic behavior, the third segment represents when the uplift and soil plasticity mechanisms are activated simultaneously, while the second one represents a transition zone where the activated mechanism may be uplift (the response is still elastic in this case), soil yielding or both of them.

The generic distribution of stresses proposed (Figs. 1 (a)-(e)) are sufficient to elaborate all the limiting curves of the (N, M) resistance domain (Fig. 3).

The elastic limit (curve 1, Fig. 3), enclosing all the possible combination of loads (N,M) leading to an elastic response of the soil-foundation system, derives from two stress distribution states, in both of them, only one point situated at the extremity of the foundation has reached the soil yielding stress σ_y (due to eccentric loading); the first state (Fig. 1 (b)) represents the case when the footing is not yet uplifted but due to the increasing of the applied load, the elastic soil under the foundation is getting more close to its yielding limit; the second state (Fig. 1 (a)) represents the case when the foundation is uplifted but the soil is still acting elastically.

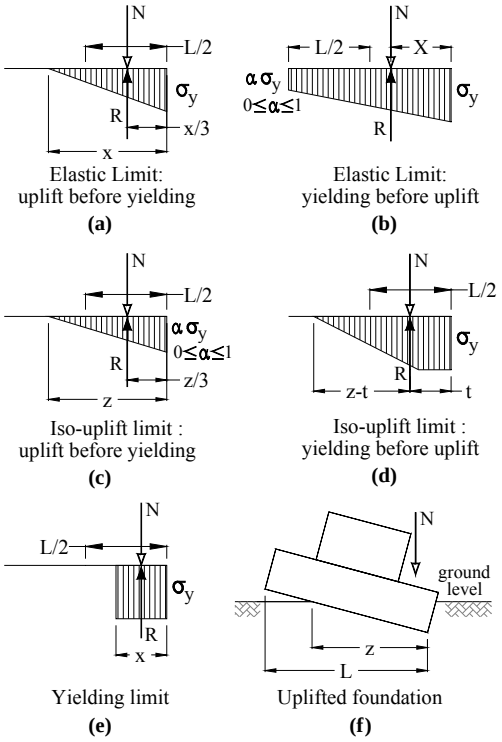

Fig. 1 (a)-(e) The proposed stresses diagram schematization for different footing states; (f) Sketch of an uplifted foundation

The intersection between the curves obtained from these two states is a point where uplift and soil yielding are generated simultaneously at the end of the elastic response phase (point A, Fig. 3).

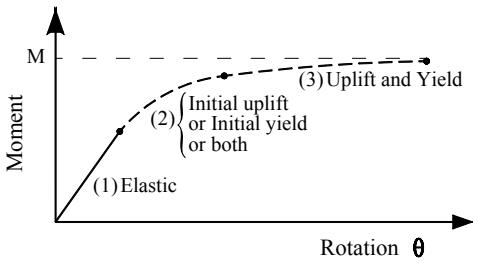

Fig. 2 The proposed schematization of the Moment-Rotation curve under monotonic loading

The failure limit (curve 3 in Fig. 3), represents the total soil plastification under the foundation area in contact with soil, the state of stress distribution corresponding to this limit is represented by Fig. 1 (e), where z represents the effective foundation length in contact with soil, the contact area with soil being (z.B).

The uplift initiation limit describing all possible combinations of load leading to an uplift initiation of the foundation (curve 2 in Fig. 3), is retrieved from a more generic case called the Iso-uplift curves, by considering that the effective foundation length "z" in contact with soil is equal to its total length L.

The Iso-uplift curves (for example curve 4 in Fig. 3), describe a generic foundation state where the foundation is uplifted and has a fixed contact length z without or with soil plastification; the corresponding states of stress distribution are represented by Figs. 1 (c) and (d) respectively. Each iso-uplift curve describes these two states and encloses all possible combinations of load leading to a fixed amount of foundation uplift. The varying iso-uplift curves are intercepted between the uplift initiation limit and the failure limit.

A. Elastic Limit

This limit represents the frontier between elastic and plastic response of the soil-foundation system. Since uplift is a non-linear elastic mechanism, the elastic limit encloses some load combinations for which uplift mechanism is activated, in this specific case, foundation uplift occurs before soil yielding and the stress distribution under the foundation corresponding to the elastic limit can be represented by Fig. 1 (a). Otherwise, when the soil-foundation system enters the plastic response phase before the activation of the uplift mechanism, the elastic limit corresponds to the stress distribution represented by Fig. 1 (b).

Considering the kinematics for these two states, the elastic limit can be expressed as follows:

1. Uplift Before Soil Yielding

If uplift occurs before soil yielding (Fig. 1 (a)): the stresses diagram has a triangular shape since stresses in tension (at the foundation's end where uplift takes place) are neglected, the maximum stress at the other end of the footing reaches the soil yielding strength σ_y. In this case, the resultant R of the stresses diagram, which is also equal to the axial load N, is given by:

$$R = \frac{1}{2}\sigma_y.B.z \tag{1}$$

Using (1), the expression of z can be written as (2), and hence, the eccentricity e of the resultant R with respect to the center of the footing can be expressed by (3).

$$z = \frac{2N}{\sigma_y.\,B} \tag{2}$$

$$e = \frac{L}{2} - \frac{2N}{3\sigma_y.B} \tag{3}$$

The expression of the moment is obtained as a function of the axial vertical load N by summing the moments about the center of the footing. Then, normalizing by $L.N_{max}$ with $N_{max}= \sigma_y$. L.B the vertical yielding force of the soil-foundation system, leads to the normalized expression of the moment, corresponding to the elastic limit when uplift is prior to soil yielding.

$$\frac{M}{LN_{max}} = \frac{1}{2}\frac{N}{N_{max}}\left[1 - \frac{4}{3}\frac{N}{N_{max}}\right] \tag{4}$$

2. Soil Yielding Before Uplift

If soil yielding is prior to uplift (Fig. 1 (b)): the maximum stress at one end of the footing reaches the soil yielding strength, σ_y, while the stress in the other end is still minor to σ_y and is considered equal to $\alpha.\sigma_y$, with α varying from 0 to 1. The expression of the eccentricity in this case is:

$$e = \frac{L}{2} - X = \frac{L}{2} - \frac{L}{3}\frac{\sigma_y(1+2\alpha)}{\sigma_y(1+\alpha)} = \frac{L}{6}\frac{(1-\alpha)}{(1+\alpha)} \tag{5}$$

and N and the normalized expression of the moment are obtained, respectively, as:

$$N = \frac{\alpha\sigma_y + \sigma_y}{2}\,BL = \frac{(1+\alpha)}{2}\,\sigma_y BL = \frac{(1+\alpha)}{2}\,N_{max} \tag{6}$$

$$\frac{M}{LN_{max}} = \frac{1}{6}\frac{N}{N_{max}}\frac{(1-\alpha)}{(1+\alpha)} = \frac{1-\alpha}{12},\ \alpha \in [0;1] \tag{7}$$

It is obvious that each of these two expressions of the moment ((4) and (7)) is valid for the interval of N/N_{max} verifying each case.

The intersection between these two curves can be retrieved from Fig. 1 (b) by putting α=0, corresponding to a foundation state where the uplift is about to initiates at one end and the soil yielding is about to initiates at the second end of the foundation. The moment expression becomes:

$$\frac{M}{LN_{max}} = \frac{1}{6}\frac{N}{N_{max}} \tag{8}$$

The equality between (4) and (8) gives the coordinates of the intersection point:

$$A\left(\frac{N}{N_{max}}=\frac{1}{2};\frac{M}{LN_{max}}=\frac{1}{12}\right)$$

Hence, the entire expression of the elastic limit is given by (9.a) and (9.b):

$$\frac{M}{LN_{max}}=\frac{1}{2}\frac{N}{N_{max}}\left[1-\frac{4}{3}\frac{N}{N_{max}}\right] \text{ for } \frac{N}{N_{max}}\in[0;0.5] \quad (9.a)$$

$$\frac{M}{LN_{max}}=\frac{1}{6}\frac{N}{N_{max}}\frac{1-\alpha}{1+\alpha}=\frac{1-\alpha}{12},\ \alpha\in[0;1] \text{ for } \frac{N}{N_{max}}\in[0.5;1] \quad (9.b)$$

B. Iso-Uplift Curves

The expression of the moment is given for a generic state (Fig. 1 (f)), as function not only of N/N_{max} but also of the ratio z/L where z represents the part of the foundation length still in contact with soil. The separation percentage of the foundation from soil is ((L-z)/L)100%.

For a specific value of the ratio z/L, two cases are identified:

1. Uplift Before Soil Yielding

If uplift occurs before soil yielding (Fig. 1 (c)): This means that uplift mechanism is activated but the soil-foundation system is still behaving elastically; and this occurs when at one end the foundation is detached from the soil, at the other end, the stress has not yet reached the soil yielding strength σ_y and is considered equal to $\alpha.\sigma_y$, with α varying from 0 to 1 for each specific value of z/L.

As a function of z/L, the expression of the eccentricity e, the axial load N and the normalized moment are expressed as:

$$e=\frac{L}{2}-\frac{z}{3} \quad (10)$$

$$N=\frac{1}{2}\alpha.\sigma_y.B.z.\frac{L}{L}=\frac{\alpha}{2}.\frac{z}{L}N_{max} \quad (11)$$

$$\frac{M}{LN_{max}}=\frac{1}{2}\frac{N}{N_{max}}\left[1-\frac{2}{3}\frac{z}{L}\right]=\frac{1}{4}\alpha\frac{z}{L}\left[1-\frac{2}{3}\frac{z}{L}\right], \text{ with } 0<z<L \quad (12)$$

This expression is valid for all the values of N/N_{max} giving elastic moment, in other words, for N/N_{max} varying from zero till the intersection of the iso-uplift curve with the elastic limit. The coordinates of this intersection point are:

$$B\left(\frac{N}{N_{max}}=\frac{1}{2}\frac{z}{L};\frac{M}{LN_{max}}=\frac{1}{4}\frac{z}{L}-\frac{1}{6}\frac{z^2}{L^2}\right)$$

Hence, for each z/L with 0<z<L, the expression of the moment is:

$$\frac{M}{LN_{max}}=\frac{1}{2}\frac{N}{N_{max}}\left[1-\frac{2}{3}\frac{z}{L}\right]=\frac{1}{4}\alpha\frac{z}{L}\left[1-\frac{2}{3}\frac{z}{L}\right]$$
$$\alpha\in[0;1] \quad \text{for}\ \frac{N}{N_{max}}\in[0;0.5z/L] \quad (13)$$

2. Soil Yielding Before Uplift

If soil plasticity is prior to uplift (Fig. 1 (d)): It's the case of combined soil yielding and foundation uplift. At one end of the footing the soil has already been plasticized, and it reached the soil yielding strength σ_y for a portion t from the foundation's extremity, with t varying between 0 and z, while on the other end uplift is activated. The expression of the eccentricity in this case is:

$$e=\frac{\frac{1}{4}Lz-\frac{1}{6}z^2+\frac{1}{4}Lt-\frac{1}{6}zt-\frac{1}{6}t^2}{\frac{1}{2}(z+t)} \quad (14)$$

The expression of the moment found in this case is valid for N/N_{max} varying from the value corresponding to the intersection of the iso-uplift curve with the elastic limit till one, and is given by:

$$\frac{M}{LN_{max}}=\frac{N}{N_{max}}\frac{1}{\frac{1}{2}\left(\frac{z}{L}+\frac{t}{L}\right)}\left[\frac{1}{4}\frac{z}{L}-\frac{1}{6}\frac{z^2}{L^2}+\frac{1}{4}\frac{t}{L}-\frac{1}{6}\frac{z}{L}\frac{t}{L}-\frac{1}{6}\frac{t^2}{L^2}\right] \quad (15)$$

with 0<z<L; and for each z/L: $N/N_{max}\in[0.5z/L;1]$, $t\in[0;z]$.

C. Initial Uplift Condition

It's the limit condition before the foundation is detached from soil. This case can be deduced from the previous one by replacing z with L (z/L=1) corresponding to a foundation that is still in full contact with soil. Hence (13) and (15) give:

When uplift occurs before soil yielding:

$$\frac{M}{LN_{max}}=\frac{\alpha}{12},\ \alpha\in[0;1] \text{ for } \frac{N}{N_{max}}\in[0;0.5] \quad (16)$$

When soil plasticity is prior to uplift:

$$\frac{M}{LN_{max}}=\frac{N}{N_{max}}\frac{1}{6}\frac{1}{\left(1+\frac{t}{L}\right)}\left[1+\frac{t}{L}-2\frac{t^2}{L^2}\right] \quad (17)$$

with $t\in[0;L]$ for $N/N_{max}\in[0.5;1]$.

D. Yielding Limit (Failure Limit)

This curve represents the failure limit corresponding to the total plastification of the soil under the foundation (Fig. 1 (e)). It discriminates between admissible and inadmissible load combinations within the soil when uplift and foundation sinking mechanisms are activated. Hence the total soil yielding under the foundation is intended to be under the effective foundation area in contact with soil. In Fig. 1 (e), the length z represents the reduced foundation length due to uplift.

The expressions, in this case, of the eccentricity and of the moment are respectively:

$$e=\frac{L}{2}-\frac{x}{2}=\frac{L}{2}\left(1-\frac{N}{\sigma_y BL}\right)=\frac{L}{2}\left(1-\frac{N}{N_{max}}\right) \quad (18)$$

$$\frac{M}{LN_{max}} = \frac{1}{2}\frac{N}{N_{max}}\left[1-\frac{N}{N_{max}}\right] \text{ with } \frac{N}{N_{max}} \in [0;1] \quad (19)$$

It is worth to note that the point of intersection of an iso-uplift (for a certain value of z/L) with that representing the failure limit is given by:

$$C\left(\frac{N}{N_{max}}=\frac{z}{L}\ ;\ \frac{M}{LN_{max}}=\frac{1}{2}\frac{z}{L}-\frac{1}{2}\frac{z^2}{L^2}\right)$$

Also, it is useful to note that the toppling of the foundation corresponding to a total separation from the soil except for an edge point, represented by segment (5) in Fig. 3, is given by the equation:

$$\frac{M}{LN_{max}} = \frac{1}{2}\frac{N}{N_{max}} \quad (20)$$

Equation (20) is derived from the condition of foundation uplift on elastic soil (M=NL/2); this is the same expression of the overturning of a rigid block on a rigid soil, and can be also found by putting z=0 in (13) representing an iso-uplift curve with a total separation condition. Segment (5) is tangent to the failure curve limit at the origin of space (N/N_{max}=0). Thus, an important aspect to retain is that, soil failure occurs before the total detachment of the foundation from the soil.

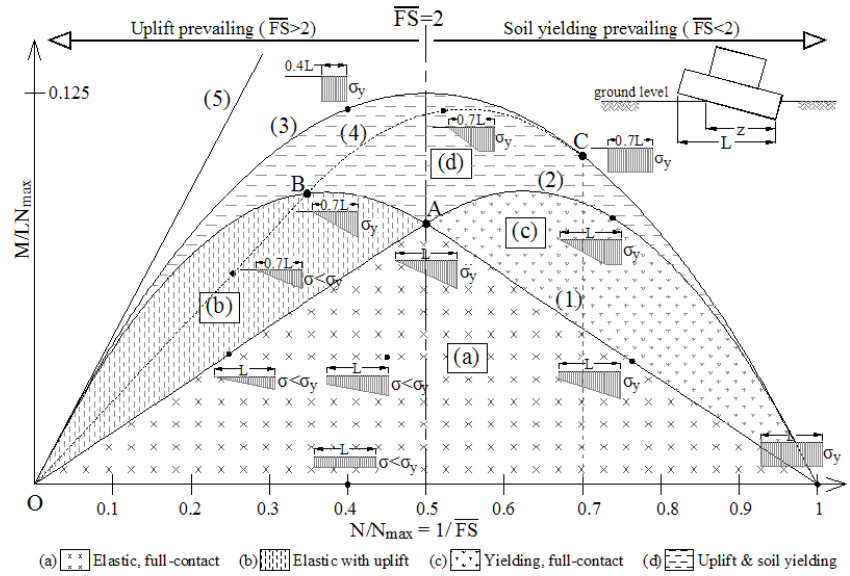

Fig. 3 Interaction curves in the normalized (N,M) plane of a rigid foundation on a rigid (curve 5) and deformable (curve 3) soil, with the different limit states curves lying within the failure limit, and with a schematization of the variation of the stresses diagram corresponding to the several foundation states

In Fig. 3, the several curves are presented with a schematization of the variation of the stresses diagram with respect to different foundation states. The Elastic limit (curve 1), the uplift initiation limit (curve 2) and the failure limit (curve 3) divide the obtained diagram in four zones characterizing the main elastic-plastic behavior of the soil-foundation system, and are described as follows:

- Zone (a): the soil-foundation response is purely elastic, and the foundation is in full-contact with the soil; none of the two non-linear mechanisms is activated yet.
- Zone (b): the soil-foundation response is still elastic, the soil has not reached its compressive yielding strength, but the foundation has initiated to uplift.
- Zone (c): the soil-foundation response is plastic. While the foundation is still in full-contact with the soil (uplift mechanism not activate) the soil has already reached its compressive yielding strength, and hence the foundation sinking mechanism is active.
- Zone (d): the soil-foundation response is plastic; both uplift and soil plasticity mechanisms are active.

This diagram can be divided also vertically into two main zones with respect to the line N/N_{max}=0.5 (where the normalized moment attains its maximum value $0{,}125N/N_{max}$).

V. Observations

It is worth to note, here, that in the case where the soil yielding strength σ_y is taken equal to the soil-foundation bearing capacity, the ratio $N/N_{max} = N/(\sigma_y BL) = N/(q_u BL)$ represents the inverse of the soil-foundation bearing capacity safety factor, FS; otherwise, in the general case, it is considered as the nominal safety factor $\overline{FS}$. It is clear from Fig. 3 that when $\overline{FS}$ is higher than 2, the uplift mechanisms occurs before soil yielding and prevails in the soil-foundation response as illustrated in Fig 4 (a), while soil plastification occurs first and prevails for value of $\overline{FS}$ lower than 2, as

illustrated in Fig 4 (b). This observation is also stated by the [6] where $FS = \overline{FS}$.

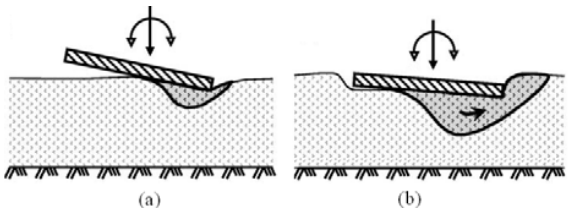

Fig. 4 (a) Foundation uplifting with limited soil plastification; uplift is the prevailing failure mechanism, (b) Foundation uplifting with extensive soil plastification; soil yielding is the predominant failure mechanism [5]

On other hand, the *i*so-uplift curves, represented in a generic way by curve (4) in Fig. 3 (curve 4 is an iso-uplift curve for z/L= 0.7), give explicitly very detailed information about the coupling relation between the two non-linear mechanisms. In fact, each iso-uplift curve is divided into two branches, one lying in the elastic non-linear zone (b) and represented by the branch OB, and another one lying in the plastic zone (d) and represented by the branch BC of the iso-uplift curve. Since the two non-linear mechanisms are activated simultaneously only in zone (d), thus talking about their coupling is meaningful exclusively in this zone. The branch BC correlates each value of the applied axial load N to a related value of the applied moment M that will cause the uplift of the foundation and the reduction of its contact area with soil from A=B.L to A'= B.z despite the soil yielding. The most important point of this curve is the one that gives the applied combined loads (N, M) leading to failure, represented by the point C, the intersection of the iso-uplift curve with the failure limit. The abscissa of this point is $N/N_{max}=z/L$.

This means that, for example, for a 30% uplifted foundation (z/L=0.7), the maximum axial load that can support the foundation before failure is $N=(z/L)\ N_{max}=0.7\ N_{max}=N'_{max}$, thus the vertical yielding force of the soil-foundation system is reduced by 30%. The ordinate of this point ($M/LN_{max}= 0.5z/L-0.5z^2/L^2$) gives explicitly the value of the moment to be applied, associated to this failure, all this is thanks to the analytic expression of the iso-uplift curves.

VI. Comparison with Existing Works in Literature

The results found analytically herein, especially for the iso-uplift curves can be of a big interest; a comparison with other works existing in the literature as that presented in [6] (Fig. 5 (a)), for instance, shows quiet a difference in the iso-uplift shape. Reference [6] shows that the uplift-plasticity coupling was treated by introducing, in the force space, an uplift surface moving inside an uplift domain, following the same idea developed for the loading surface moving inside the failure surface, and then super-imposed the surfaces of iso-uplift with the failure criterion. Reference [6] shows that the two mechanisms were treated separately and an hyperbolic shape of the iso-uplift surfaces was postulated, with presumption based on FE simulations as shown in Fig. 5 (b); then [6] suggested that their coupling can be understood by supper-imposing them in the same plane of forces. In fact, the part of the iso-uplift surfaces lying out the failure limit has no sense, and the intersection of the iso-uplift curves with the failure limit is underestimated in this assumption, especially for low amount of foundation uplift. For example, the first iso-uplift representing uplift initiation limit (δ=0% in Fig. 5 (a)) is shown intercepting the (N,M) failure limit by a point having a moment different from zero and a vertical force smaller that the vertical yielding force, this is in contradiction with reality, since for a zero uplift, the maximum vertical force that can support the foundation is equal to the vertical yielding force while the moment correlated to this axial force on the failure limit is obviously zero.

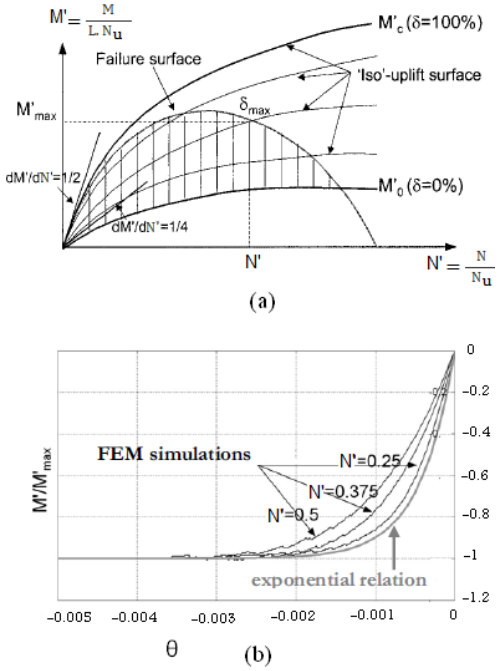

Fig. 5 (a) Iso-uplift surface and failure criterion in the normalized (M,N) plane after [6] (b)Relationship between moment and rocking angle using numerical simulations with the code Dynaflow, after [6]

In Fig. 3, the analytically constructed (N, M) domain shows this intersection as ($N/N_{max}=1$; $M/LN_{max}=0$) for the uplift initiation curve, while for an iso-uplift curve with a percentage of soil-foundation separation δ=((L-z)/L)100%, the intersection is given by: ($N/N_{max}=z/L$; $M/LN_{max}= 0.5z/L-0.5z^2/L^2$).

In the work presented herein, the coupling between the two mechanisms is obtained automatically by means of a unique analytical expression of the moment in the (M, N) plane, and the iso-uplift curve is obtained from the integration of the stresses distribution under the foundation for a determined and discrete foundation state where uplift or/and soil yielding mechanisms are activated respectively/simultaneously; the shape and the end point of the iso-uplift curves seem to

represent in a more accurate way the realistic behavior of the soil-foundation system, and the coupling between uplift and soil yielding is more elaborated especially near the failure limit.

VII. Comparison with Experimental Results

Analytically, the normalized expression of the moment is found as given by (19):

$$\frac{M}{LN_{max}} = 0.5\frac{N}{N_{max}}\left(1-\frac{N}{N_{max}}\right)$$

which is a parabola intercepting the axis of normalized axial forces in points (0,0) and (1,0) and having an initial slope 0.5 at the origin of space. The peak normalized moment given by this expression is M_{max}/LN_{max}= 0.125, corresponding to $N=0.5N_{max}$.

Experimental results and numerical analysis existing in the literature show similar expressions of the failure limit with different values for the initial slope μ_m, and sometimes with the introduction of a parameter β controlling the form of the curve and of its slope at point (1, 0).

The general expression of these failure limits is of the form:

$$\frac{M}{LN_u} = \mu_m \frac{N}{N_u}\left(1-\left(\frac{N}{N_u}\right)^{\beta}\right) \quad (21)$$

where $N_u=q_uBL$ represents the vertical static bearing force of the foundation.

TABLE I
Values of the Parameters Controlling the Expression of the Failure Limit in the Plane (N,M) Normalized by Nu, Resulting from Various Experimental and Numerical Analyses Existing in Literature

Reference	Type of tests	μ_m	β
[7]	Experimental tests	0.35	1
[8]	Experimental tests	0.38	0.94
[9]	Experimental tests	0.33	0.95
[10]	Experimental tests	0.36	1
[13]	Numerical analysis	0.34	1

Table I gives the different values of μ_m and β found by several authors. The value of the peak moment, established from these tests and from other more sophisticated ones on dense and loose sand and on clay is about: M_{max}/LN_u=0.0875. It's worth to note that all these tests were performed with superficial (not embedded) foundations. Reference [3] found that the peak normalized moment load of 0.1 was representative of model footing tests lying on sand. Results presented in [7] and [11] for strip footings suggest a lower peak value of 0.0875. In [11] also it was found that the size of the normalized failure surface increased with footing embedment and suggested that the peak is M_{max}/LN_{max}=0.125 at w/D=0.5 (w: embedment depth, D: foundation diameter). Sand density and footing roughness were found not to affect the N-M failure surface. Results on sideswipe tests in [12] gave M_{max}/LN_u=0.09. The numerical analyses conducted in [13] on superficial foundation lying on non-cohesive soil led to a peak of 0.085. More recently, several swipe tests on embedded foundations had shown again an increase in the size of the yield surface, hence an increase in the peak (M_{max}/LN_u) value. Indeed, [14] and [15] found a peak value almost equal to 0.1 for w/D=0.5 (w: embedment depth, D: foundation diameter).

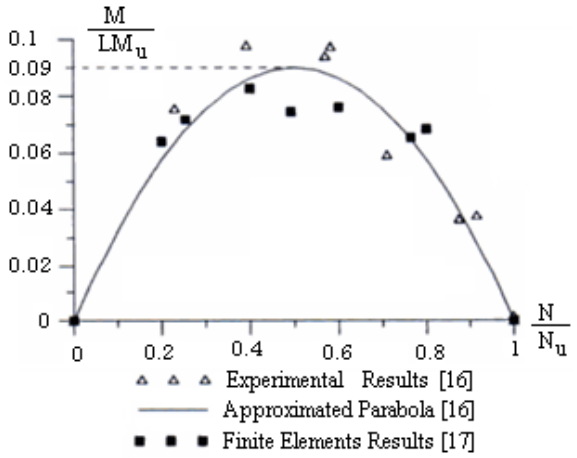

Fig. 6 Normalized plot of experimental failure loads of a strip footing on sand [17]

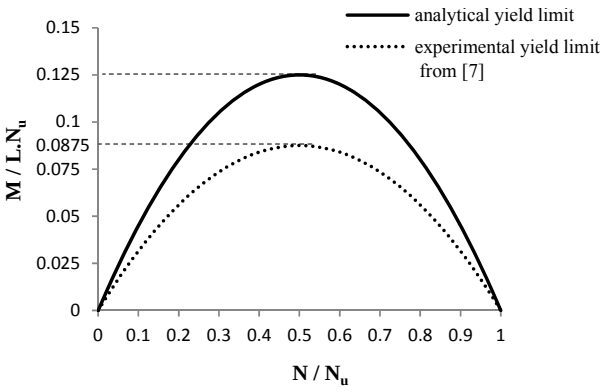

Fig. 7 The failure limit obtained experimentally by [7] and that obtained analytically normalized by the vertical bearing force N_u

Figs. 6 and 7 show that the peak values between analytical results and experimental ones [7], [16], [17] are not very far away one of the other, especially observing the several results obtained for embedded foundations, and considering that in civil engineering domain it's very rare to encounter structures with not embedded foundations. From the other hand, the non-unicity of the peak value resulting from experimental results sheds the light, on the precautionary approximation done by the several authors in order to construct the failure limit, based on an evident dispersed series of experimental data (Fig. 6).

Acknowledgment

This research has received funding from the European Community's Seventh Framework Programme (FP7/2007-

2013) under grant agreement n° 244229 (www.perpetuate.eu).

REFERENCES

[1] K. Terzaghi, "*Theoretical soil mechanics*", J. Willey, New York, 1943.
[2] J.Brinch-Hansen, "A revised and extended formula for bearing capacity", *Danish geotechnical institute*,Copenhagen, Bulletin No.28, pp. 5-11, 1970.
[3] R. Butterfield, J. Ticof, "The use of physical models in design (discussion)", Proceedings, 7th European Conference on Soil Mechanics and Foundation Engineering, Brighton, UK, Vol.4, pp. 259-261, 1979.
[4] R. Butterfield, "A simple analysis of load capacity of rigid footings on granular media", Journée de Géotechnique, pp. 128-134, 1980.
[5] N. Gerolymos, G. Gazetas, "Development of Winkler model for static and dynamic response of caisson foundations with soil and interface nonlinearities", Soil Dynamics and Earthquake Engineering, Vol.26, pp. 363-376, 2006a.
[6] C. Crémer, A. Pecker, L. Davenne, "Cyclic macroelement for soil-structure interaction: material and geometrical nonlinearities", International Journal for Numerical and Analytical Methods in Geomechanics, Vol.25, pp. 1257-1284, 2001.
[7] R. Butterfield, G. Gottardi, "A complete three-dimensional failure envelope for shallow footings on sand", Géotechnique, Vol.44, No.4, pp. 181, 1994.
[8] J. Ticof, "Surface footings on sand under general planar loads", PhD Thesis, University of Southampton, UK, 1977.
[9] L. Montrasio, R. Nova, "Un modello di calcolo degli assestamenti di fondazioni superficiali sottoposte all'azione di carichi eccentrici ed inclinati", Atti del convegno su "Deformazioni dei terreni ed interazione terreno-struttura in condizioni di esercizio", Monselice, Vol.2, pp. 141-152, 1998b.
[10] G. Gottardi, "Modellazione del comportamento di fondazioni superficiali su sabbia soggette a diverse condizioni di carico", Ph.D. Thesis, University of Padova, Italy, 1992.
[11] R. Nova, L. Montrasio, "Settlements of shallow foundations on sand: Geometric effects", Geotechnique, Vol.47, No.1, pp. 49-60, 1997.
[12] G. Gottardi, G. T. Houlsby, "Model tests of circular footings on sand subjected to combined laods", Department of Engineering Science, Oxford University, Oxford, OUEL 2071/95, 1995.
[13] R. Bovolenta, F. Schiaffino, R. Berardi, "Sulla valutazione della stabilità di fondazioni superficiali sottoposte a condizioni generali di carico", Fondazioni superficiali e profonde, *5th National conference of geotechnical engineering researchers*, Bari, 2006.
[14] B.W. Byrne, G.T. Houlsby, "Observations of footing behavior on loose carbonate sands", Géotechnique Vol. 51, No. 5, pp. 463-466, 2001.
[15] L. Govoni, S. Gouvernec, G. Gottardi,, "Centrifuge modelling of circular shallow foundations on sand", International Journal of Physical Modelling in Geotechnics, Vol.10, No.2, pp. 35–46, 2010.
[16] G. Gottardi, R. Butterfield, "On the bearing capacity of surface footings on sand under general planar load", Soils and Foundations, Vol. 33, No.3, pp. 68–79, 1993.
[17] L. Zdravkovic, , P.M. Ng, D.M. Potts, "Bearing capacity of surface foundations on sand subjected to combined loading", Numerical methods in geotechnical engineering, Mestat ed.,Presses de l'ENPC/LCPC, Paris, pp. 323-330, 2002.